Simulation of Heat and Chemical Reactions on Peristaltic Flow of a Williamson Fluid in an Inclined Asymmetric Channel

Nadeem, Sohail*+

Department of Mathematics, Quaid-i-Azad University 45320, Islamabad 44000, PAKISTAN

Akram, Safia

Department of Humanities and Basic Sciences, Military College of Signals, National University of Sciences and Technology, Rawalpindi 46000, PAKISTAN

Akbar, Noreen Sher

DBS&H, CEME, Nathonal University of Sciences and Technology, Islamabad, PAKISTAN

ABSTRACT: *This work concerns the peristaltic flow of a Williamson fluid model in an inclined asymmetric channel under combined effects of heat and mass transfer. The governing nonlinear partial differential equations are simplified under the lubrication approach and then solved analytically and numerically. The analytical results are computed with the help of regular perturbation and the numerical results are found by using shooting method.*

KEY WORDS: *Williamson fluid, Peristaltic flow, Heat and mass transfer, Perturbation solution, Numerical solution.*

INTRODUCTION

During the last few decades, the study of non-Newtonian fluids become more important because of its variety of applications in engineering and Biomechanics. A few of these applications include food mixing and chyme movement in the intestine, flow of plasma, flow of blood-a Bingham fluid, flow of nuclear fuel slurries, flow of liquid metals and alloys, flow of mercury amalgams and lubrication with heavy oils and greases. Due to complexity of non-Newtonian fluids there are many models of non-Newtonian fluids. An extensive study of these non-Newtonian fluid models is available in the refs [1-8]. To be more specific heat and mass transfer analysis in peristaltic mechanism plays important role in a number of scientifically and engineering applications. The combined effects of heat and mass transfer in a moving fluid usually describes the relations between the fluxes and the driving potentials [9] . Further, the mass fluxes can also be created by temperature gradients and this is the Soret or thermal diffusion effect. In general, the thermal-diffusion and diffision-Thermo effects are of smaller order of

* *To whom correspondence should be addressed.*
+ *E-mail: snqau@hotmail.com*
1021-9986/13/2/93 15/$/3.50

magnitude than the effects described by Fourier's or Fick law and are often neglected in heat and mass transfer processes [10]. The effects of heat and mass transfer in peristaltic flows of Newtonian and non-Newtonian problems are carried by *Nadeem & Akbar* in their papers [11-13]. To the beat of authors knowledge only a limited attention has been focussed to the study of combined effects of heat and mass transfer in the peristaltic flow problems. The present investigation discuss the combined effects of heat and mass transfer on the peristaltic flow of a Williamson fluid model in an asymmetric channel. The governing equations of Williamson fluid model along with heat and mass transfer equations are reduced under the assumptions of long wavelength. The reduced equations are then solved subject to the boundary conditions of asymmetric channel with the help of regular perturbation method and numerically by shooting technique. At the end, the physical feature of the pertinent parameters of interest are discussed in detail.

MATHEMATICAL FORMULATION

Let us consider the peristaltic transport of an incompressible Williamson fluid in a two dimensional inclined channel of width $d_1 + d_2$. The flow is generated by sinusoidal wave trains propagating with constant speed c along the channel walls. The geometry of the wall surface is defined as

$$Y = H_1 = d_1 + a_1 \cos\left[\frac{2\pi}{\lambda}(X - ct)\right], \quad \text{upper wall} \tag{1}$$

$$Y = H_2 = -d_2 - b_1 \cos\left[\frac{2\pi}{\lambda}(X - ct) + \varphi\right], \quad \text{lower wall}$$

Where a_1 and b_1 are the amplitudes of the waves, λ is the wave length, $d_1 + d_2$ is the width of the channel, c is the velocity of propagation, t is the time and X is the direction of wave propagation, the phase difference φ varies in the range $0 \le \varphi \le \pi$, $\varphi = 0$ corresponds to symmetric channel with waves out of phase and $\varphi = \pi$ the waves are in phase, and further a_1, b_1, d_1, d_2 and φ satisfies the condition

$$a_1^2 + b_1^2 + 2a_1 b_1 \cos\varphi \le (d_1 + d_2)^2$$

The equations governing the flow of a Williamson fluid in the presence of gravity effects are

$$\frac{\partial U}{\partial X} + \frac{\partial V}{\partial Y} = 0 \tag{2}$$

$$\rho\left(\frac{\partial U}{\partial t} + U\frac{\partial U}{\partial X} + V\frac{\partial U}{\partial Y}\right) = \tag{3}$$

$$-\frac{\partial P}{\partial X} + \frac{\partial \tau_{XX}}{\partial X} + \frac{\partial \tau_{XY}}{\partial Y} + \rho g \sin\alpha$$

$$\rho\left(\frac{\partial V}{\partial t} + U\frac{\partial V}{\partial X} + V\frac{\partial V}{\partial Y}\right) = \tag{4}$$

$$-\frac{\partial P}{\partial Y} + \frac{\partial \tau_{XY}}{\partial X} + \frac{\partial \tau_{YY}}{\partial Y} - \rho g \cos\alpha$$

Heat and mass transfer equations are

$$C'\left(\frac{\partial T}{\partial t} + U\frac{\partial T}{\partial X} + V\frac{\partial T}{\partial Y}\right) = \tag{5}$$

$$\frac{K'}{\rho}\nabla^2 T + \tau_{XX}\frac{\partial U}{\partial X} + \tau_{XY}\left(\frac{\partial V}{\partial X} + \frac{\partial U}{\partial Y}\right) + \tau_{YY}\frac{\partial V}{\partial Y}$$

$$\frac{\partial C}{\partial t} + U\frac{\partial C}{\partial X} + V\frac{\partial C}{\partial Y} = \tag{6}$$

$$D\left(\frac{\partial^2 C}{\partial X^2} + \frac{\partial^2 C}{\partial Y^2}\right) + \frac{DK_T}{T_m}\left(\frac{\partial^2 T}{\partial X^2} + \frac{\partial^2 T}{\partial Y^2}\right)$$

where

$$\nabla^2 = \frac{\partial^2}{\partial X^2} + \frac{\partial^2}{\partial Y^2}$$

In which U, V are the velocities in X and Y directions in fixed frame, ρ is constant density, P is the pressure, ν is the kinematic viscosity, g is the acceleration due to gravity, K' is the thermal conductivity, C' is the specific heat, T is the temperature, D is the coefficient of mass diffusivity, T_m is the mean temperature, K_T is the thermal diffusion ratio and C is the concentration of fluid.

The constitutive equation for the extra stress tensor τ for Williamson fluid model is [4].

$$\boldsymbol{\tau} = \left[\mu_\infty + (\mu_0 + \mu_\infty)(1 - \Gamma\dot{\gamma})^{-1}\right]\dot{\gamma}, \tag{7}$$

In which - PI is the spherical part of the stress due to constraint of incompressibility, τ is the extra stress tensor, μ_∞ is the infinite shear rate viscosity, μ_0 is the zero shear rate viscosity, Γ is the time constant and $\dot{\gamma}$ is defined as

$$\dot{\gamma} = \sqrt{\frac{1}{2}\sum_i\sum_j \dot{\gamma}_{ij}\dot{\gamma}_{ji}} = \sqrt{\frac{1}{2}\Pi} \tag{8}$$

Here Π is the second invariant strain tensor. We consider the constitutive Eq. (7), the case for which $\mu_\infty = 0$ and $\Gamma\dot{\gamma} < 1$. The component of extra stress tensor therefore, can be written as

$$\boldsymbol{\tau} = \mu_0\left[(1-\Gamma\dot{\gamma})^{-1}\right]\dot{\gamma} = \mu_0\left[(1+\Gamma\dot{\gamma})\right]\dot{\gamma} \tag{9}$$

Introducing a wave frame (x,y) moving with velocity c away from the fixed frame (X,Y) by the transformation

$$x = X - ct,\ y = Y,\ u = U - c,\ v = V, \tag{10}$$

$$\text{and}\ \ P(x) = P(X,t)$$

Defining

$$\bar{x} = \frac{x}{\lambda},\ \bar{y} = \frac{y}{d_1},\ \bar{u} = \frac{u}{c},\ \bar{v} = \frac{v}{c},\ \bar{t} = \frac{ct}{\lambda}, \bar{h}_1 = \frac{h_1}{d_1}, \tag{11}$$

$$d = \frac{d_2}{d_1}\ \ a = \frac{a_1}{d_1},\ \ b = \frac{b_1}{d_1}, \bar{h}_2 = \frac{h_2}{d_2},\ \ \bar{\tau}_{\bar{x}\bar{x}} = \frac{\lambda}{\mu_0 c}\tau_{xx},$$

$$\bar{\tau}_{\bar{x}\bar{y}} = \frac{d_1}{\mu_0 c}\tau_{xy}, \bar{\tau}_{\bar{y}\bar{y}} = \frac{d_1}{\mu_0 c}\tau_{yy},\ Fr = \frac{C^2}{gd_1},\ \theta = \frac{T-T_0}{T_1-T_0},$$

$$\delta = \frac{d_1}{\lambda},\ \ Re = \frac{\rho c d_1}{\mu_0},\ \ We = \frac{\Gamma c}{d_1},\ \ P = \frac{d_1^2}{c\lambda\mu_0}\bar{P}, \bar{\dot{\gamma}} = \frac{\dot{\gamma} d_1}{c},$$

$$Ec = \frac{c^2}{C'(T_1-T_0)}, Pr = \frac{\rho\nu C'}{K'}, M = \sqrt{\frac{\sigma}{\upsilon}}B_0 d,\ \ \Phi = \frac{C-C_0}{C_1-C_0}$$

Using the above non-dimensional quantities and the resulting equations in terms of stream function Ψ(dropping the bars, $u = \frac{\partial\Psi}{\partial y}$, $v = -\delta\frac{\partial\Psi}{\partial x}$) can be written as

$$\delta Re\left[\left(\Psi_y\frac{\partial}{\partial x} - \Psi_x\frac{\partial}{\partial y}\right)\Psi_y\right] = \tag{12}$$

$$-\frac{\partial P}{\partial x} + \delta^2\frac{\partial\tau_{xx}}{\partial x} + \frac{\partial\tau_{xy}}{\partial y} + \frac{Re}{Fr}\sin\alpha$$

$$-\delta^3 Re\left[\left(\Psi_y\frac{\partial}{\partial x} - \Psi_x\frac{\partial}{\partial y}\right)\Psi_x\right] = \tag{13}$$

$$-\frac{\partial P}{\partial y} + \delta^2\frac{\partial\tau_{xy}}{\partial x} + \delta\frac{\partial\tau_{yy}}{\partial y} - \delta\frac{Re}{Fr}\cos\alpha$$

$$Re\,\delta\left(\Psi_y\theta_x - \Psi_x\theta_y\right) = \frac{1}{Pr}\left(\theta_{yy} + \delta^2\theta_{xx}\right) + \tag{14}$$

$$Ec(\delta^2\left(\tau_{xx}\Psi_{xy} - \tau_{xy}\Psi_{xx}\right) + \tau_{xy}\Psi_{yy} - \delta\tau_{yy}\Psi_{xy})$$

$$Re\,\delta\left(\Psi_y\Phi_x - \Psi_x\Phi_y\right) = \tag{15}$$

$$\frac{1}{Sc}\left(\delta^2\Phi_{xx} + \Phi_{yy}\right) + Sr\left(\delta^2\theta_{xx} + \theta_{yy}\right)$$

where

$$\tau_{xx} = 2\left[1 + We\dot{\gamma}\right]\frac{\partial^2\Psi}{\partial x\partial y}, \tag{16}$$

$$\tau_{xy} = \left[1 + We\dot{\gamma}\right]\left(\frac{\partial^2\Psi}{\partial y^2} - \delta^2\frac{\partial^2\Psi}{\partial x^2}\right),$$

$$\tau_{yy} = -2\delta\left[1 + We\dot{\gamma}\right]\frac{\partial^2\Psi}{\partial x\partial y},$$

$$\dot{\gamma} = \left[2\delta^2\left(\frac{\partial^2\Psi}{\partial x\partial y}\right)^2 + \left(\frac{\partial^2\Psi}{\partial y^2} - \delta^2\frac{\partial^2\Psi}{\partial x^2}\right)^2 + 2\delta^2\left(\frac{\partial^2\Psi}{\partial x\partial y}\right)^2\right]^{1/2}$$

In which δ, Re, We represent the wave, Reynolds and Weissenberg numbers, respectively. Under the assumptions of long wavelength δ<<1 and low Reynolds number, neglecting the terms of order δ and higher, Eqs. (12) to (16) take the form

$$\frac{\partial P}{\partial x} = \frac{\partial}{\partial y}\left[\left(1 + We\frac{\partial^2\Psi}{\partial y^2}\right)\frac{\partial^2\Psi}{\partial y^2}\right] + \frac{Re}{Fr}\sin\alpha = 0 \tag{17}$$

$$\frac{\partial P}{\partial y} = 0 \tag{18}$$

$$\frac{\partial^2\theta}{\partial y^2} = -Pr\,Ec\left[\left(\frac{\partial^2\Psi}{\partial y^2}\right)^2 + We\left(\frac{\partial^2\Psi}{\partial y^2}\right)^3\right] \tag{19}$$

$$\frac{1}{Sc}\frac{\partial^2\Phi}{\partial y^2} + Sr\frac{\partial^2\theta}{\partial y^2} = 0 \tag{20}$$

Elimination of pressure from Eqs. (17) and (18), yield

$$\frac{\partial^2}{\partial y^2}\left[\left(1 + We\frac{\partial^2\Psi}{\partial y^2}\right)\frac{\partial^2\Psi}{\partial y^2}\right] = 0 \tag{21}$$

$$\frac{\partial^2\theta}{\partial y^2} = -Pr\,Ec\left[\left(\frac{\partial^2\Psi}{\partial y^2}\right)^2 + We\left(\frac{\partial^2\Psi}{\partial y^2}\right)^3\right] \tag{22}$$

$$\frac{1}{Sc}\frac{\partial^2\Phi}{\partial y^2} + Sr\frac{\partial^2\theta}{\partial y^2} = 0 \tag{23}$$

The instantaneous volume flow rate in the fixed frame is defined as

$$Q = \int_{H_2}^{H_1} U(X, Y, t)\, dY \tag{24}$$

In the wave frame the rate of volume flow presented as

$$q = \int_{h_1}^{h_2} u(x, y)\, dy \tag{25}$$

In which h_1 and h_2 are the functions of x only. From Eqs. (10), (24) and (25) we obtain

$$Q = q + ch_1(x) - ch_2(x) \tag{26}$$

The time mean flow over a period T at a fixed position X is defined as

$$\bar{Q} = \frac{1}{T}\int_0^T Q\, dt \tag{27}$$

Making use of (26) into (27) and after integrating, we get

$$\bar{Q} = q + cd_1 - cd_2 \tag{28}$$

The dimensionless time-mean flows Θ in the laboratory frame and F in the wave frame are defined as

$$\Theta = \frac{\bar{Q}}{cd_1},\ F = \frac{q}{cd_1} \tag{29}$$

Therefore, Eq. (28) can be written as

$$\Theta = F + 1 + d \tag{30}$$

in which

$$F = \int_{h_2(x)}^{h_1(x)} \frac{\partial \Psi}{\partial y}\, dy = \Psi(h_1(x)) - \Psi(h_2(x)) \tag{31}$$

$$h_1(x) = 1 + a\cos 2\pi x,\ h_2(x) = -d - b\cos(2\pi x + \varphi) \tag{32}$$

The corresponding boundary conditions are

$$\Psi = \frac{F}{2} \text{ at } y = h_1 = 1 + a\cos 2\pi x, \tag{33}$$

$$\Psi = -\frac{F}{2} \text{ at } y = h_2 = -d - b\cos(2\pi x + \varphi),$$

$$\frac{\partial \Psi}{\partial y} = -1 \text{ at } y = h_1,$$

$$\frac{\partial \Psi}{\partial y} = -1 \text{ at } y = h_2$$

$$\theta = 0,\ \Phi = 0 \text{ at } y = h_1 \tag{34}$$

$$\theta = 1,\ \Phi = 1 \text{ at } y = h_2$$

Solution of the problem

Since Eq. (21) is highly non linear, therefore, the exact solution of Eq. (21) seems to be impossible. Adopting the similar procedure as done by *Nadeem & Akram* [4], the solution of Eq. (21) straight forward can be written as

$$\Psi = \frac{F + h_1 - h_2}{(h_2 - h_1)^3}\left(2y^3 - 3(h_1 + h_2)y^2 + 6h_1h_2y\right) - y + \tag{35}$$

$$\frac{1}{(h_2 - h_1)^3}\left(\left(\frac{F}{2} + h_1\right)\left(h_2^3 - 3h_1h_2^2\right) - \left(h_2 - \frac{F}{2}\right)\left(h_1^3 - 3h_2h_1^2\right)\right) +$$

$$We\left(A + By + A_{11}\frac{y^2}{2!} + B_1\frac{y^3}{3!} + A_1\frac{y^4}{4!}\right)$$

where

$$A = \tag{36}$$

$$-\frac{6}{(h_2 - h_1)^3}\left(\frac{A_1}{4!}\left(h_1^3(2h_2 - h_1) - h_2^3(2h_1 - h_2)\right)\right)\left(\frac{h_1h_2^2}{2} - \frac{h_2^3}{6}\right)$$

$$-\frac{A_1}{3!}\left(\frac{h_1^2h_2^2}{2} + \frac{h_1h_2^3}{2} - \frac{h_2^4}{4}\right),$$

$$= \frac{A_1h_1h_2}{2}\times$$

$$\left(\frac{(h_1 + h_2)}{3} - \frac{1}{2(h_2 - h_1)^3}\left(h_1^3(2h_2 - h_1) - h_2^3(2h_1 - h_2)\right)\right),$$

$$= A_1\times$$

$$\left(\frac{(h_1 + h_2)}{4(h_2 - h_1)^3}\left(h_1^3(2h_2 - h_1) - h_2^3(2h_1 - h_2)\right) - \frac{(h_1^2 + h_1h_2 + h_2^2)}{3!}\right),$$

$$= \frac{12}{(h_2 - h_1)^3}\left(\frac{A_1}{4!}\left(h_1^3(2h_2 - h_1) - h_2^3(2h_1 - h_2)\right)\right),$$

$$= -288\left(\frac{F + h_1 - h_2}{(h_2 - h_1)^3}\right)^2$$

The axial pressure gradient is obtained from Eq. (17)

$$\frac{dP}{dx} = \frac{12(F + h_1 - h_2)}{(h_2 - h_1)^3} + \frac{Re}{Fr}\sin\alpha + \tag{37}$$

$$We\left(-\frac{12}{(h_2 - h_1)^3}\frac{A_1}{4!}\left(h_1^3(2h_2 - h_1) - h_2^3(2h_1 - h_2)\right) -\right.$$

$$\left.144(h_1 + h_2)\left[\frac{F + h_1 - h_2}{(h_2 - h_1)^3}\right]^2\right)$$

The solution of Eqs. (22) and (23) with the help of Eq. (35) can be written as

$$\theta = -Br\left(\frac{1}{60}\left(\frac{a_0}{(h_1-h_2)^6}y^2 - \frac{a_1}{(h_1-h_2)^6}y^3 + \frac{a_2}{(h_1-h_2)^6}y^4 + + \frac{a_3}{(h_1-h_2)^3}y^5 + \frac{1}{2}A_1^2We^2y^6\right)\right. + We\left(\frac{1}{2240}\left(y^2\left(\frac{a_4}{(h_1-h_2)^9} - \frac{a_5}{(h_1-h_2)^9}y + \frac{a_6}{(h_1-h_2)^9}y^2 - \frac{a_7}{(h_1-h_2)^9}y^3 + \frac{a_8}{(h_1-h_2)^6}y^4 + \frac{a_9}{(h_1-h_2)^3}y^5 + 5A_1^3We^3y^6\right)\right)\right) + c_1y + c_2 \quad (38)$$

$$\Phi = SrScBr\left(\frac{1}{60}\left(\frac{a_0}{(h_1-h_2)^6}y^2 - \frac{a_1}{(h_1-h_2)^6}y^3 + \frac{a_2}{(h_1-h_2)^6}y^4 + \frac{a_3}{(h_1-h_2)^3}y^5 + \frac{1}{2}A_1^2We^2y^6\right)\right. + We\left(\frac{1}{2240}\left(y^2\left(\frac{a_4}{(h_1-h_2)^9} - \frac{a_5}{(h_1-h_2)^9}y + \frac{a_6}{(h_1-h_2)^9}y^2 - \frac{a_7}{(h_1-h_2)^9}y^3 + \frac{a_8}{(h_1-h_2)^6}y^4 + \frac{a_9}{(h_1-h_2)^3}y^5 + 5A_1^3We^3y^6\right)\right)\right) + c_3y + c_4 \quad (39)$$

$$c_1 = \frac{1}{6720(h_1-h_2)^9}\left(112(h_1-h_2)^3(-60(h_1-h_2)^5 + (h_1^3(a_2+a_3h_1^4) + h_1^2(a_2-2a_3h_1^4)h_2 + h_1(a_2+a_3h_1^4)h_2^2 + a_2h_2^3 - a_3h_1^2h_2^5 + 2a_3h_1h_2^6 - a_3h_2^7 + a_0(h_1+h_2) - a_1(h_1^2+h_1h_2+h_2^2))Br) + b_0BrWe + b_1BrWe^2 + b_2BrWe^4\right) \quad (40)$$

$$c_2 = \frac{1}{6720(h_1-h_2)^9}\left(h_1(6720(h_1-h_2)^8 - 112(h_1-h_2)^3h_2(a_0 - a_1(h_1+h_2) + a_3(h_1-h_2)^3(h_1+h_2)(h_1^2+h_2^2) + a_2(h_1^2+h_1h_2+h_2^2))Br - b_3BrWe - b_4BrWe^2 + b_5BrWe^4)\right)$$

$$c_3 = \frac{-ScSr}{6720(h_1-h_2)^9}\left(112(h_1-h_2)^3(60(h_1-h_2)^5 + (h_1^3(a_2+a_3h_1^4) + h_1^2(a_2-2a_3h_1^4)h_2 + h_1(a_2+a_3h_1^4)h_2^2 + a_2h_2^3 - a_3h_1^2h_2^5 + 2a_3h_1h_2^6 - a_3h_2^7 + a_0(h_1+h_2) - a_1(h_1^2+h_1h_2+h_2^2))Br) + b_0BrWe + b_1BrWe^2 + b_2BrWe^4\right), \quad (41)$$

$$c_4 = \frac{ScSr}{6720(h_1-h_2)^9}\left(h_1(112(h_1-h_2)^3(60(h_1-h_2)^5 + h_2(a_0 - a_1(h_1+h_2) + a_3(h_1-h_2)^3(h_1+h_2)(h_1^2+h_2^2) + a_2(h_1^2+h_1h_2+h_2^2))Br + b_3BrWe + b_4BrWe^2 + b_5ScSrBrWe^4)\right),$$

Where the constants appearing in Eqs. (40) and (41) are defined in appendix.

EXPERSSIONS FOR DIFFERENT WAVE SHAPE

The non-dimensional expressions for three considered wave form are given as

1) Sinusoidal wave

$$h_1(x) = 1 + a\sin 2\pi x, \quad h_2(x) = -d - b\sin(2\pi x + \varphi).$$

2) Multisinusoidal wave

$$h_1(x) = 1 + a\sin 2n\pi x, \quad h_2(x) = -d - b\sin(2n\pi x + \varphi).$$

3) Triangular wave

$$h_1(x) = 1 + a\left[\frac{8}{\pi^3}\sum_{m=1}^{\infty}\frac{(-1)^{m+1}}{(2m-1)^2}\sin\left(2\pi(2m-1)x\right)\right],$$

$$h_2(x) = -d - b\left[\frac{8}{\pi^3}\sum_{m=1}^{\infty}\frac{(-1)^{m+1}}{(2m-1)^2}\sin\left(2\pi(2m-1)x + \varphi\right)\right]$$

5) Trapezoidal wave

$$h_1(x) = 1 + a\left[\frac{32}{\pi^2}\sum_{m=1}^{\infty}\frac{\sin\frac{\pi}{8}(2m-1)}{(2m-1)^2}\sin\left(2\pi(2m-1)x\right)\right],$$

$$h_2(x) = -d - b\left[\frac{32}{\pi^2}\sum_{m=1}^{\infty}\frac{\sin\frac{\pi}{8}(2m-1)}{(2m-1)^2}\sin\left(2\pi(2m-1)x + \varphi\right)\right]$$

Table 1: Comparison of velocity profile for (a) We=0.3, (b) We=0.6 other parameters are d=1, b=0.7, a=0.7, $\varphi=\pi/2$, Re = 0.4 Fr=0.5, s x = 0, Θ= 0.2.

R	Perturb sol, We=0.3	Numer sol, We=0.3	Perturb sol, We=0.6	Numer sol, We=0.6
-1.0	-1.00000	-1.00000	-1.00000	-1.00000
-0.7	-0.81659	-0.76807	-0.81659	-0.71669
-0.4	-0.71667	-0.64131	-0.71667	-0.66498
-0.1	-0.66498	-0.57779	-0.66490	-0.64290
0.2	-0.64290	-0.54742	-0.64290	-0.64242
0.5	-0.64242	-0.54665	-0.64242	-0.64242
0.8	-0.66345	-0.57313	-0.66345	-0.66345
1.1	-0.71397	-0.63697	-0.71397	-0.71393
1.4	-0.81328	-0.76275	-.081328	-0.81328
1.7	-1.00000	-1.00000	-1.00000	-1.00000

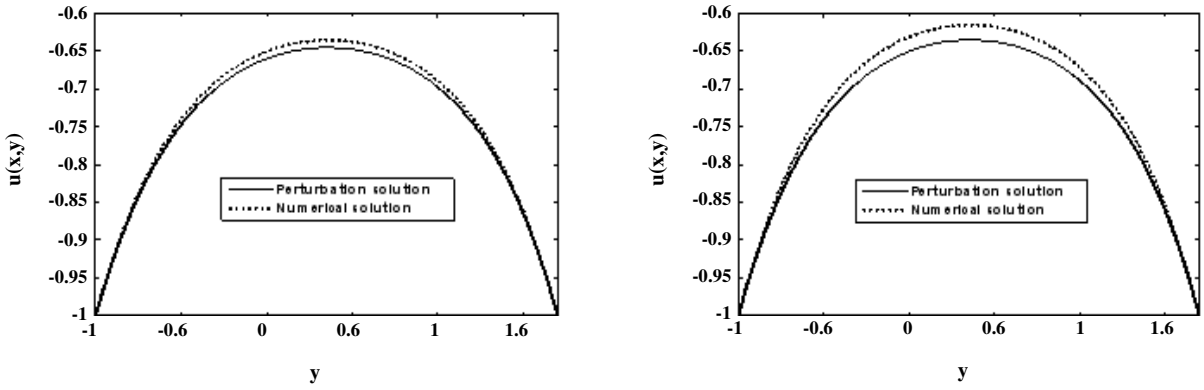

Fig. 1: Comparison of velocity profile for (a) We = 0.3, (b) We = 0.6 other parameters are d=1, b=0.7, a = 0.7, $\varphi=\pi/2$, Re = 0.4, Fr = 0.5, α = 0.2, x = 0, Θ= 0.2.

Numerical solution

To get the numerical solution of the velocity profile we solved the Eq. (21) with the relevant boundary conditions given in Eq. (33) by employing shooting method. The comparitive study is also made to see the validity of the results.

RESULTS AND DISCUSSION

In this section numerical and graphical results of the problem under consideration are discussed. Figs. 1(a) and 1(b) and Table 1 shows the comparison of velocity profile. The expression for the pressure rise and pressure gradient is calculated using a mathematics software Mathematica. In order to see the variation of pressure rise with volume flow rate Θ for different values of width of channel a, Froude number Fr, amplitude ratio φ and Reynolds number Re, Figs. 2 to 5 are presented. It is observed from Fig. 2 that the pumping rate increases with an increase in width of the channel a in the retrograde ($\Delta P > 0$, $\Theta < 0$) and peristaltic pumping ($\Delta P > 0$, $\Theta > 0$) regions, while pumping rate decreases in the copumping ($\Delta P < 0$, $\Theta > 0$) region with an increase in width of the channel a. From Fig. 3 it is seen that with an increase in Froude number Fr, the pumping rate decreases in all the regions. Fig. 4 shows the variation of pressure rise with volume flow rate Θ for different values of amplitude ratio φ. It is observed that in the retrograde ($\Delta P > 0$, $\Theta < 0$) and peristaltic pumping ($\Delta P > 0$, $\Theta > 0$) regions, the pumping rate decreases with an increase

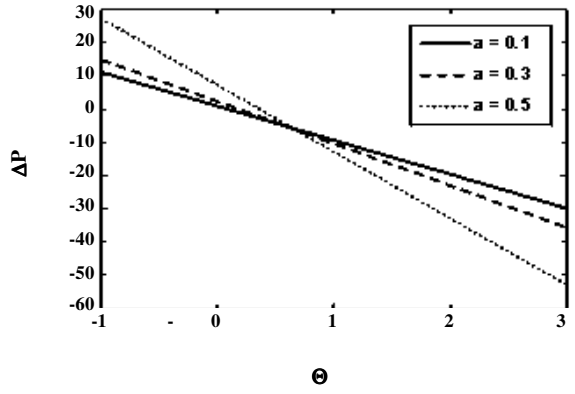

Fig. 2: Variation of ΔP with Θ for different values of a for fixed d=0.1, b=0.2, φ=π/2, We=0.03, Re=0.4, Fr=0.5, α=0.2.

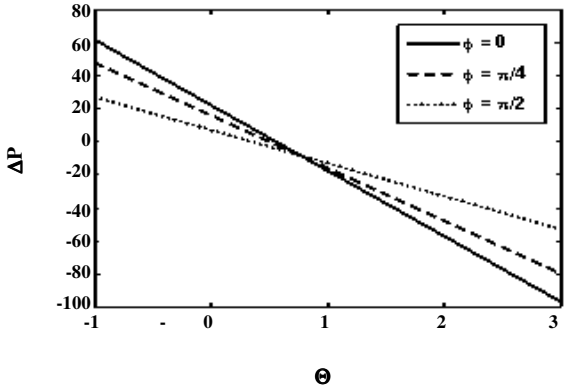

Fig. 4: Variation of ΔP with Θ for different values of φ for fixed d=0.1, b=0.2, a=0.7, We=0.03, Re=0.4, Fr=0.5, α=0.2.

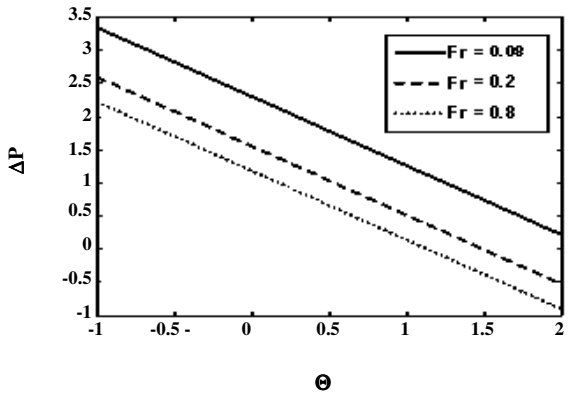

Fig. 3: Variation of ΔP with Θ for different values of Fr for fixed d=2, a=0.7, b=1.2, φ=π/2, We=0.03, Re=0.5, α=0.2.

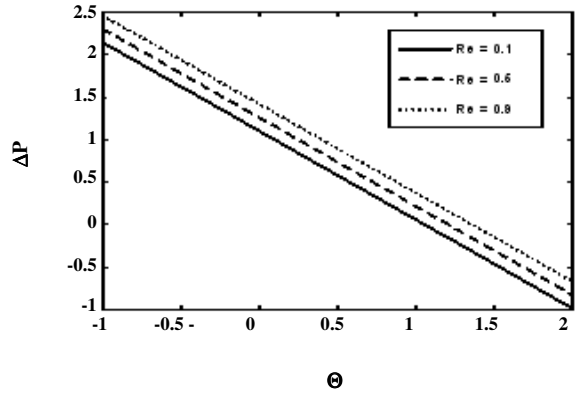

Fig. 5: Variation of ΔP with Θ for different values of Re for fixed d=2, a=0.7, b=1.2, φ=π/2, We=0.03, Fr=0.5, α=0.2.

in amplitude ratio φ, while the behavior is quite opposite in the copumping (ΔP < 0 , Θ > 0) region, here pumping rate increases with an increase in amplitude ratio φ. It is depicted from Fig. 5 that the pressure rise increases with an increase in Reynolds number Re in all the regions. The pressure gradient for different values of width of the channel a inclination angle α, Froude number Fr and amplitude ratio φ are shown in Figs. 6 to 9.

Figs. 10 to 12 show the temperature profile for different values of Brinkmann number Br, volume flow rate Θ and Weissenberg number We. It is observed from Figs. 10 and 11 that the temperature profile increases with an increase in Brinkmann number Br and volume flow rate Θ. Fig. 12 shows the temperature profile for different values of Weissenberg number We. It is observed that the temperature profile increases with an increase in Weissenberg number We when y∈[-1.5,0], while the behavior of temperature profile is opposite when y∈[0,1.5], here temperature profile decreases with an increase in Weissenberg number We. Futhermore, the maximum temperature occurs at y = 0. The concentration profile for different values of Brinkmann number Br, volume flow rate Θ, Soret number Sr, Schmidt number Sc and Weissenberg number We. It is observed that the concentration profile decreases with an increase in Brinkmann number Br, volume flow rate Θ Soret number Sr and Schmidt number Sc (see Figs. 13 to 15). It is observed from Fig. 16 that the concentration profile decreases with an increase Weissenberg number when y∈[-1.5,0], while the behavior of concentration profile is opposite when y∈[0,1.5], here concentration profile increases with an increase in Weissenberg number We. Futher the maximum concentration occurs at y = 0.

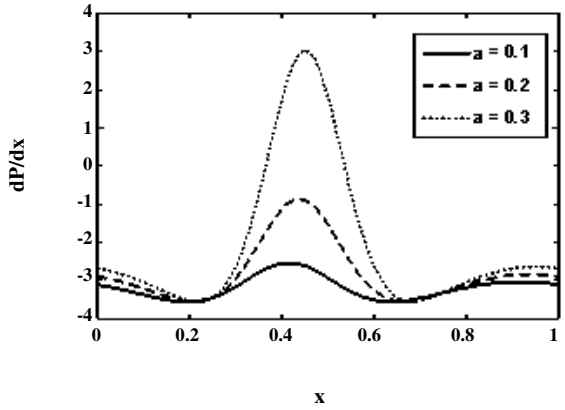

Fig. 6: Variation of dP/dx with x for different values of a for fixed d=0.1, Re=0.4, b=0.2, φ=π/4, We=0.03, Fr=0.5, Θ=0.4, α=0.2.

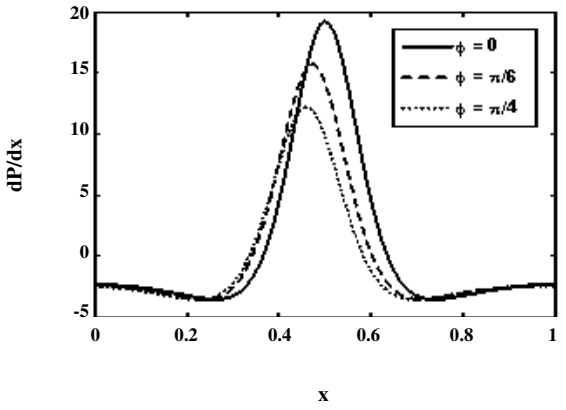

Fig. 9: Variation of dP/dx with x for different values of φ for fixed d=0.1, Re=0.4, b=0.2, Fr=0.5, We=0.03, Θ=0.4, α=0.1, a=0.4.

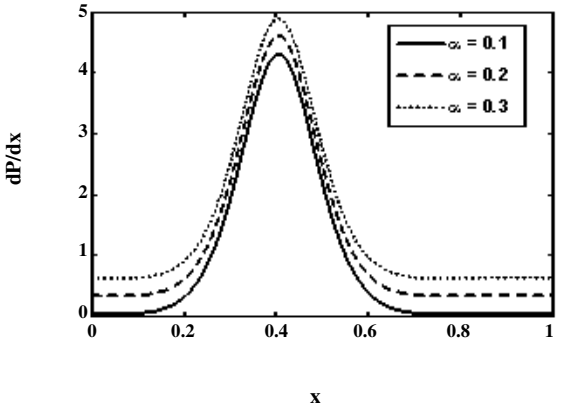

Fig. 7: Variation of dP/dx with x for different values of α for fixed d=2, Re=1.5, b=1.2, φ=π/4, We=0.03, Fr=0.5, a=0.4, Θ=0.4.

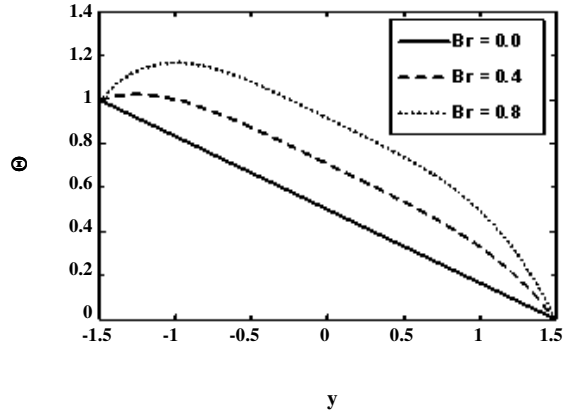

Fig. 10: Temperature profile for different values of Br for fixed d=1.5, b=1.2, We=0.03, φ=π/2, Θ=2, a=0.5, x=0.

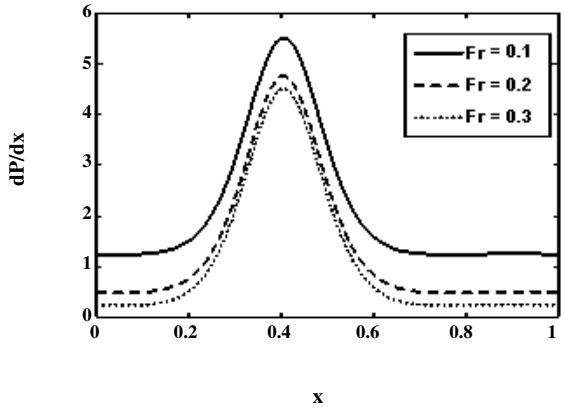

Fig. 8: Variation of dP/dx with x for different values of Fr for fixed d=2, Re=2, b=1.2, φ=π/4, We=0.03, Θ=0.4, α=0.1, a=0.4.

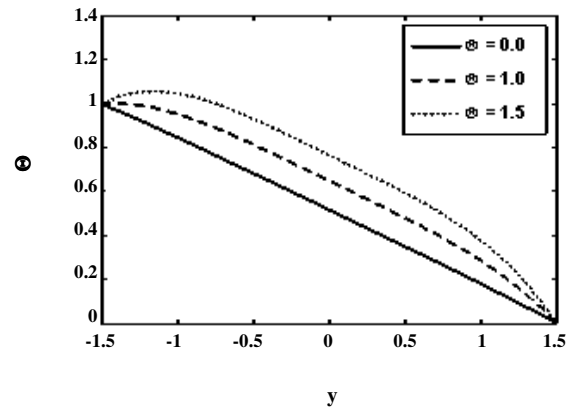

Fig. 11: Temperature profile for different values of Θ for fixed d=1.5, b=1.2, We=0.03, Br=0.8, φ=π/2, a=0.5, x=0.

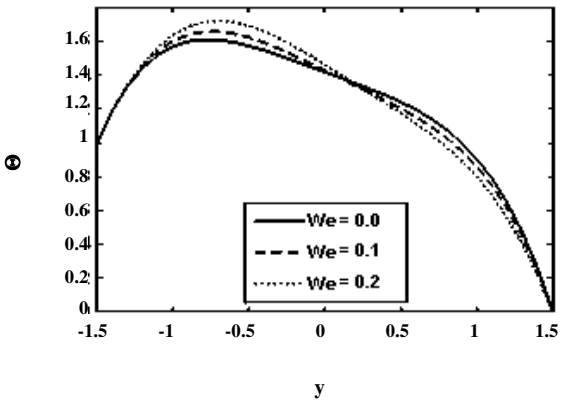

Fig. 12: Temperature profile for different values of We for fixed d=1.5, b=1.2, Br=0.8, Θ=3, φ=π/2, a=0.5, x=0.

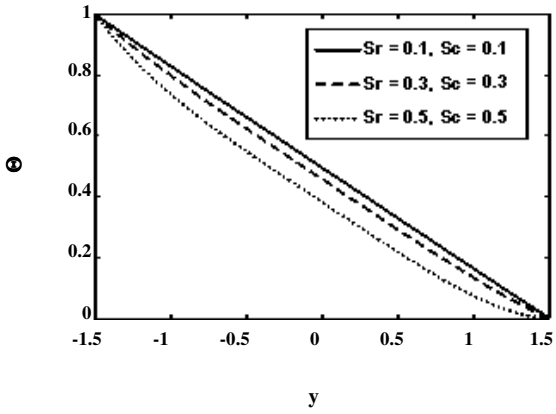

Fig. 15: Concentration profile for different values of Sr and Sc for fixed d=1.5, b=1.2, Θ=2, Br=0.9, φ=π/2, a=0.5, We=0.03, x=0.

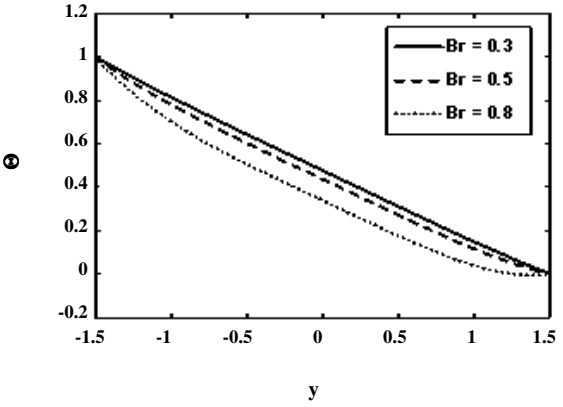

Fig. 13: Concentration profile for different values of Br for fixed d=1.5, b=1.2, Sc=0.8, Sr=0.6, Θ=2, φ=π/2, a=0.5, We=0.03, x=0.

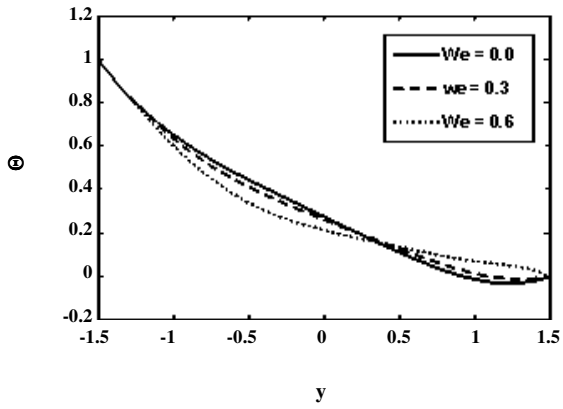

Fig. 16: Concentration profile for different values of We for fixed d=1.5, b=1.2, Sc=0.8, Sr=0.6, Br=0.9, Θ=2, φ=π/2, a=0.5, x=0.

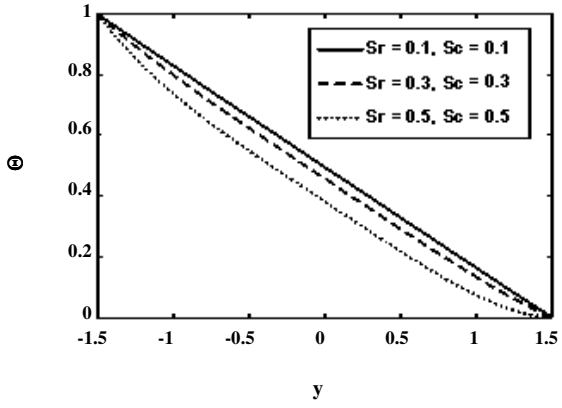

Fig. 14: Concentration profile for different values of Θ for fixed d=1.5, b=1.2, Sc=0.8, Sr=0.6, Br=0.9, φ=π/2, a=0.5, We=0.03, x=0.

Stream lines for different values of volume flow rate Θ, Weissenberg number We and width of the channel are shown in Figs. 17 to 19. It is observed from Fig. 17 that the size of the trapping bolus increases with an increase in volume flow rate Θ. It is observed from Fig. 18 that the size of the trapped bolus decreases in the upper half of the channel, while the size of the trapping bolus increases in the lower half of the channel with an increase in Weissenberg number We. Fig. 19 shows the stream lines for different values of width of the channel a. It is observed the size of the trapping bolus increases in the upper half of the channel and decreases in the lower half of the channel with an increase in width of the channel a. Fig. 20 shows the stream lines for different wave forms.

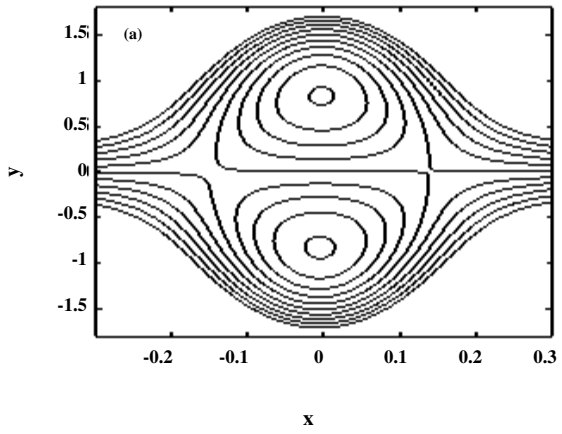

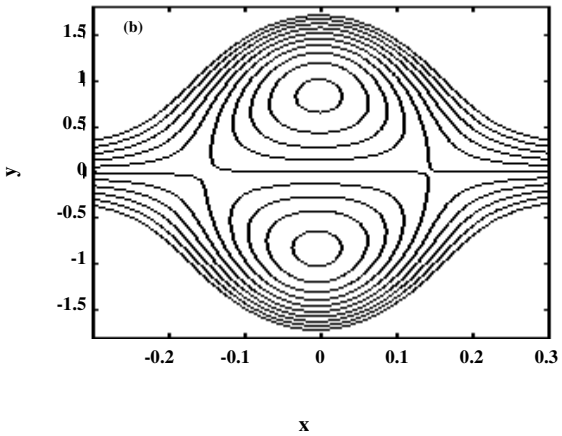

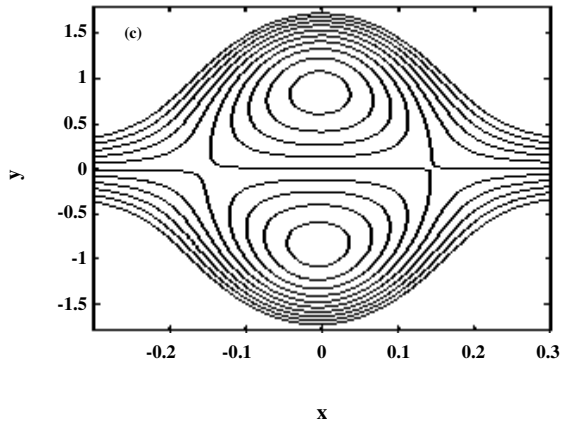

Fig. 17: Stream lines for different values of Θ Fig. (a) Θ = 0.7, Fig. (b) Θ = 0.71, Fig. (c) Θ = 0.72. The other parameters are d = 1.0, b = 0.5, φ = 0.05, a = 0.5, We = 0.01.

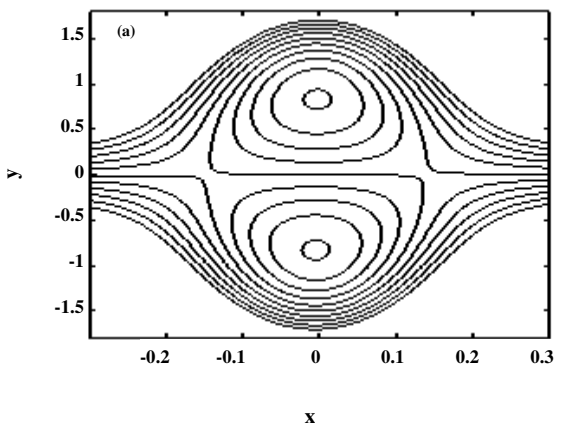

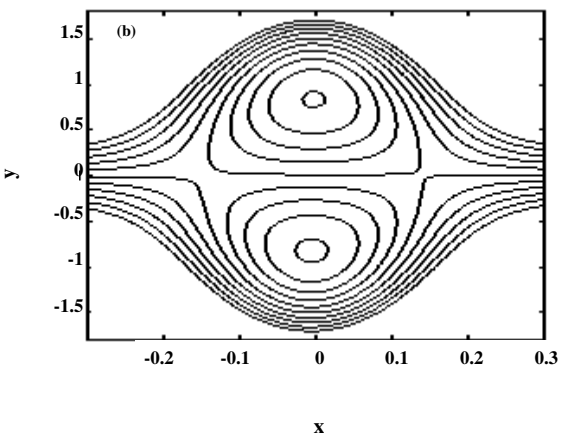

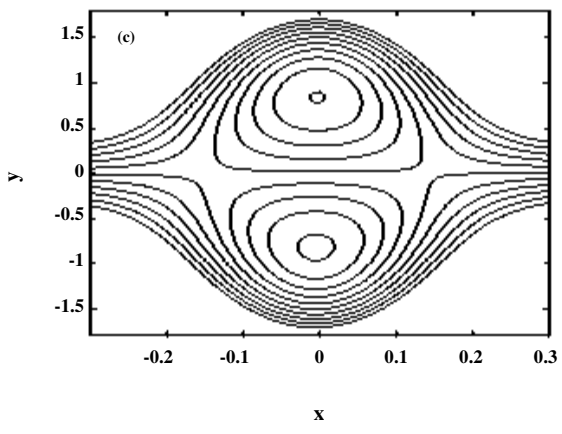

Fig. 18: Stream lines for different values of We Fig. (a) We = 0, Fig. (b) We= 0.02, Fig. (c) We= 0.04. The other parameters are d = 1.0, b = 0.5, φ = 0.05, a = 0.5, Θ = 0.7.

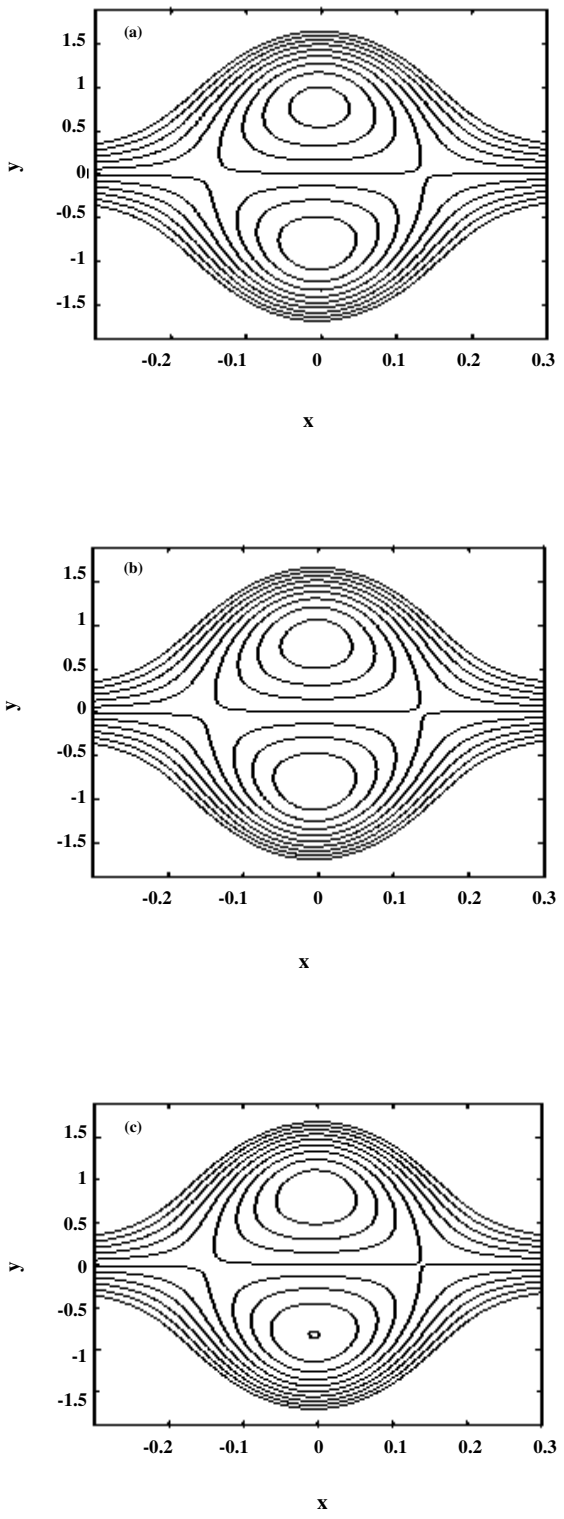

Fig. 19: Stream lines for different values of a Fig. (a) a = 0.47, Fig. (b) a = 0.48, Fig. (c) a = 0.49. The other parameters are d = 1.0, b = 0.5, φ = 0.05, We = 0.01, Θ = 0.7.

The results of pressure rise for differnt values of amplitude ratio φ and Froude number Fr are tabulated in Tables 2 and 3. It is observed from the tables that the pressure rise decreases for small values of amplitude ratio φ and increases for large values of amplitude ratio φ. Moreover the pressure rise decreases for all values of volume flow rate Θ with an increase in Froude number Fr. The results of velocity field against different values of volume flow rate Θ and Weissenberg number We are tabulated in Tables 4 and 5. It is observed from the tables that the magnitude value velocity profile decreases with an increase in volume flow rate Θ, while the velocity profile increases with an increase in Weissenberg number We for small values of y and for large values of y the behavior is quite opposite.

Nomenclature

U,V	Velocity components in X and Y direction in fixed frame
u,v	Velocity components in x and y directions in wave frame
ρ	Constant density
p	pressure
C'	Thermal diffusion ratio
K'	Thermal conductivity
M	Hartmann number
Br	Brinkmann number
Pr	Prandtl number
Re	Reynolds number
Sc	Schmidt number
Sr	Soret number
g	Acceleration due to gravity
D_m	Coefficient of Mass diffusivity
K_T	Thermal Diffusion
T	Temperature of Fluid in dimension from

Symbols

θ	Temperature of fluid in dimensionless form
C	Concentration of fluid in dimension form
Φ	Concentration of fluid in dimensionless form
φ	Amplitude ratio
a_1, b_1	Amplitude of waves
λ	Wave length
c	Velocity of propagation
Q	Volume flow rate
δ	Long wave length

Table 2: Variation of pressure rise with volume flow rate Θ for different values of φ for fixed d = 0.1, b = 0.2, a = 0.7, We = 0.03, Re = 0.4, Fr = 0.5, α = 0.2.

Θ	ΔP		
f	o	r	
	φ = 0	φ = π/4	φ = π/2
-1	5.01107	3.71505	1.8825
-0.5	4.04992	2.96007	1.43264
0	3.08877	2.20509	0.982793
0.5	2.12762	1.45011	0.532942
1	1.16648	0.695127	0.0830902
1.5	0.205329	-0.0598529	-0.366761
2	-0.755819	-0.814833	-0.816613
2.5	-1.71697	-1.56981	-1.26646

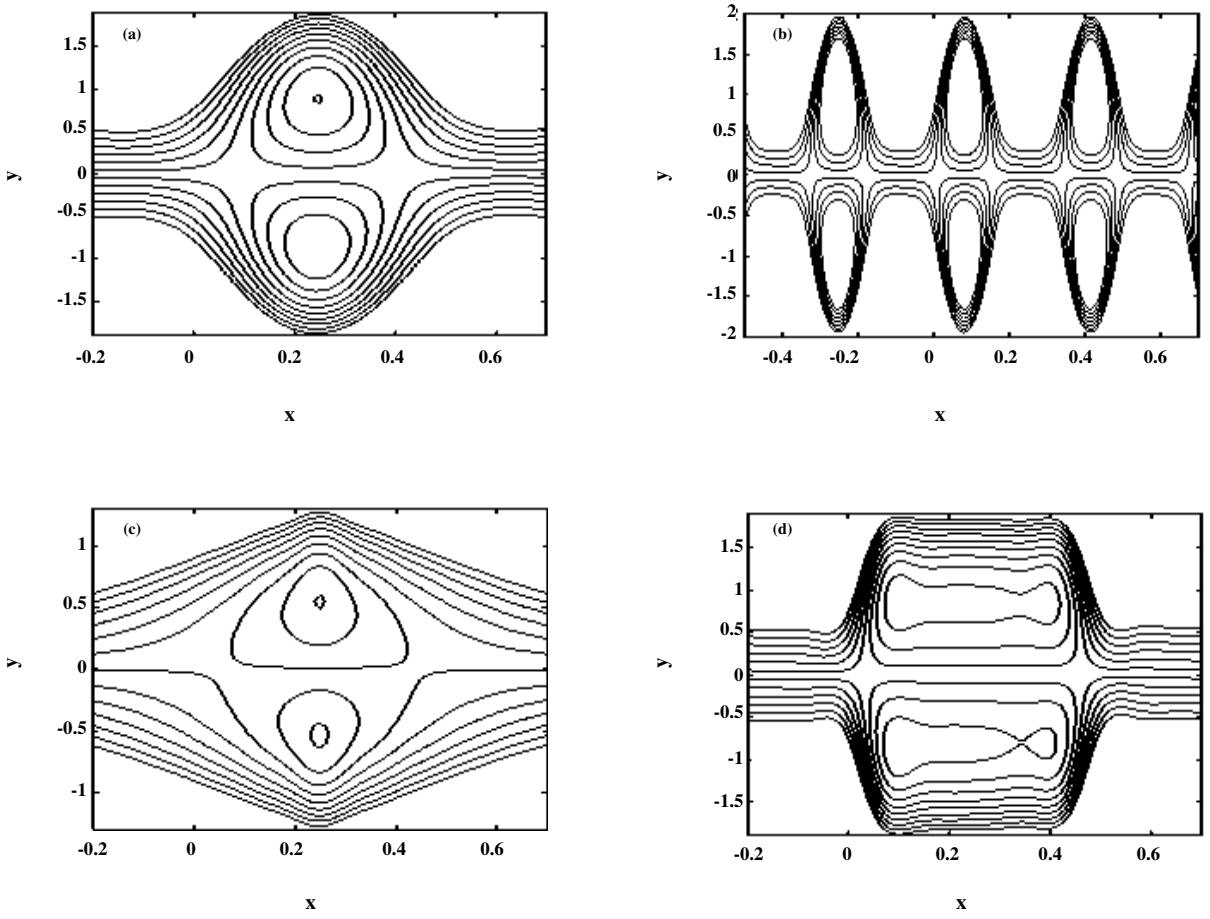

Fig. 20: Stream lines for different wave forms. Fig. (a) sinusoidal wave, Fig. (b) Multisinusoidal wave, Fig. (c) triangular wave, Fig.(d) trapezoidal wave. The other parameters are d = 1.0, b = 0.5, φ = 0.05 a = 0.5, Θ = 0.7, We = 0.01.

Table 3: Variation of pressure rise with volume flow rate Θ for different values of Fr for fixed d = 2, a = 0.7, b = 1.2, φ = π/3, We = 0.03, Re = 0.5 α = 0.2.

Θ	ΔP		
f	o	r	
	Fr = 0.08	Fr = 0.2	Fr = 0.8
-1	4.07198	3.32697	2.95447
-0.5	3.42881	2.6838	2.3113
0	2.78565	2.04064	1.66813
0.5	2.14248	1.39747	1.022496
1	1.49931	0.754299	0.381794
1.5	0.856141	0.111131	-0.261374

Table 4: Velocity profile for different values of Θ for fixed d = 1, b = 0.7, a = 0.7, We = 0.03, x = 0, φ = 0.

Θ	u(x,y)		
f	o	r	
	Θ = 0	Θ = 0.2	Θ = 0.4
-1.7	-1	-1	-1
-1.5	-0.864974	-0.845971	-0.827039
-1.3	-0.746388	-0.710623	-0.674974
-1.1	-0.644329	-0.59407	-0.543949
-0.9	-0.558885	-0.496427	-0.434109
-0.7	-0.490145	-0.417809	-0.345599
-0.5	-0.438194	-0.35833	-0.278564
-0.3	-0.403122	-0.318105	-0.23315
-0.1	-0.385016	-0.297247	-0.2095
0.1	-0383964	-0.295873	-0.20776
0.3	-0.400053	-0.314096	-0.228076
0.5	-0.433371	-0.35203	-0.270591
0.7	-0.484006	-0.409791	-0.335451
0.9	-0.552045	-0.487493	-0.422801
1.1	-0.637576	-0.58525	-0.532786
1.3	-0.740687	-0.703177	-0.665551
1.5	-0.861466	-0.841389	-0.821241

Table 5: Velocity profile for different values of We for fixed d = 1, b = 0.7, a = 0.7, Θ = 0.5, x = 0, φ = 0.

Θ	u(x,y)		
f	o	r	
	We = 0	We = 0.3	We = 0.5
-1.7	-1	-1	-1
-1.5	-0.81437	-0.846675	-0.868211
-1.3	-0.651944	-0.704434	-0.739436
-1.1	-0.512721	0.574908	-0.616366
-0.9	-0.396703	-0.459697	-0.501693
-0.7	-0.303888	-0.360421	-0.39811
-0.5	-0.234276	-0.278696	-0.308306
-0.3	-0.187869	-0.216136	-0.23498
-0.1	-0.164665	-0.174357	-0.180818
0.1	-0.164665	-0.154974	-0.648513
0.3	-0.187869	-0.159602	-0.140758
0.5	-0.234276	-0.189857	-0.160245
0.7	-0.303888	-0.247354	-0.209665
0.9	-0.396703	-0.333708	-0.291712
1.1	-0.512721	-0.450535	-0.409077
1.3	-0.651944	-0.599448	-0.564452
1.5	-0.81437	-0.782065	-0.760529

Ψ	Stream function
Fr	Froude number
α,Θ	Inclination angle of channel and magnetic field respectively
T_0	Temperature at upper wall
T_1	Temperature at lower wall
τ	Extra stress tensor

Appendix

$$b_0 = 3\left(h_1^3\left(a_6 - a_7h_1 + a_8h_1^5 + a_9h_1^9\right) + h_1^2\left(a_6 - h_1\left(a_7 + 2a_8h_1^4 + 5a_9h_1^8\right)\right)\right)h_2 + \left(a_6 - a_7h_1 + a_8h_1^5 + 10a_9h_1^9\right) + \left(a_6 - a_7h_1 - 10a_9h_1^9\right)h_2^3 - \left(a_7 - 5a_9h_1^8\right)h_2^4 - a_9h_1^7h_2^5 - a_8h_1^2h_2^6 - h_1h_2^7\left(-2a_8 + a_9h_1^4\right) - \left(a_8 - 5a_9h_1^4\right)h_2^8 - 10a_9h_1^3h_2^9 + 10a_9h_1^2h_2^{10} - 5a_9h_1h_2^{11} + a_9h_2^{12} + a_4\left(h_1 + h_2\right) - a_5\left(h_1^2 + h_1h_2 + h_2^2\right)\right)$$

$$b_1 = 56A_1^2\left(h_1 - h_2\right)^9\left(h_1 + h_2\right)\left(h_1^2 - h_1h_2 + h_2^2\right)\times \left(h_1^2 + h_1h_2 + h_2^2\right)$$

$$b_2 = 15A_1^3\left(h_1 - h_2\right)^9\left(h_1 + h_2\right)\left(h_1^2 + h_2^2\right)\left(h_1^4 + h_2^4\right)$$

$$b_3 = 3h_2\left(a_4 + h_1^2\left(a_6 - a_7h_1 + a_8h_1^5 + a_9h_1^9\right) + h_1\left(a_6 - h_1\left(a_7 + 2a_8h_1^4 + 5a_9h_1^8\right)\right)\right)h_2 + \left(a_6 - a_7h_1 + a_8h_1^5 + 10a_9h_1^9\right)h_2^2 + \left(a_7 + 10a_9h_1^8\right)h_2^3 - 5a_9h_1^7h_2^4 - h_1^2\left(a_8 - a_9h_1^4\right)h_2^5 - h_1\left(-2a_8 + a_9h_1^4\right)h_2^6 - \left(a_8 - 5a_9h_1^4\right)h_2^7 - 10a_9h_1^3h_2^8 + 10a_9h_1^2h_2^9 - 5a_9h_1h_2^{10} + a_9h_2^{11} - a_5\left(h_1 + h_2\right)\right)$$

$$b_4 = 56A_1^2\left(h_1 - h_2\right)^9h_2\left(h_1^4 - h_1^3h_2 + h_1^2h_2^2 + h_1h_2^3 + h_2^4\right)$$

$$b_5 = 15A_1^3h_2\left(-h_1 + h_2\right)^9\times \left(h_1^6 + h_1^5h_2 + h_1^4h_2^2 + h_1^3h_2^3 + h_1^2h_2^4 + h_1h_2^5 + h_2^6\right)$$

$$a_0 = 30\left(6\left(F+h_1-h_2\right)\left(h_1+h_2\right)+A_{11}\left(h_1-h_2\right)^3 We\right)^2$$

$$a_1 = 20\left(6\left(F+h_1-h_2\right)\left(h_1+h_2\right)+A_{11}\left(h_1-h_2\right)^3 We\right)^2 \times$$

$$\left(12\left(F+h_1-h_2\right)-B_1\left(h_1-h_2\right)^3 We\right)$$

$$a_2 = 5\left(144\left(F+h_1-h_2\right)^2 +\right.$$

$$6\left(h_1-h_2\right)^3\left(F+h_1-h_2\right)\left(-4B_1+A_1\left(h_1-h_2\right)\right)We +$$

$$\left.\left(A_1A_{11}+B_1^2\right)\left(h_1-h_2\right)^6 We^2\right)$$

$$a_3 = 3A_1We\left(-12\left(F+h_1-h_2\right)+B_1\left(h_1-h_2\right)^3 We\right)$$

$$a_4 = 1120\left(6\left(F+h_1-h_2\right)\left(h_1+h_2\right)+A_{11}\left(h_1-h_2\right)^3 We\right)^3$$

$$a_5 = 1120\left(6\left(F+h_1-h_2\right)\left(h_1+h_2\right)+A_{11}\left(h_1-h_2\right)^3 We\right)^2 \times$$

$$\left(12\left(F+h_1-h_2\right)-B_1\left(h_1-h_2\right)^3 We\right)$$

$$a_6 = 280\left(6\left(F+h_1-h_2\right)\left(h_1+h_2\right)+A_{11}\left(h_1-h_2\right)^3 We\right)\times$$

$$\left(288\left(F+h_1-h_2\right)\right)^2+6\left(h_1-h_2\right)^3\left(F+h_1+h_2\right)\times$$

$$\left(-8B_1+A_1\left(h_1+h_2\right)\right)We+\left(A_1A_{11}+2B_1^2\right)\left(h_1-h_2\right)^6 We^2\Big)$$

$$a_7 = 112\left(12\left(F+h_1-h_2\right)-B_1\left(h_1-h_2\right)^3 We\right)\times$$

$$\left(144\left(F+h_1-h_2\right)^2+6\left(h_1-h_2\right)^3\left(F+h_1-h_2\right)\times\right.$$

$$\left.\left(-4B_1+3A_1\left(h_1+h_2\right)\right)We+\left(3A_1A_{11}+B_1^2\right)\left(h_1-h_2\right)^6 We^2\right)$$

$$a_8 = 56A_1We\left(288\left(F+h_1-h_2\right)^2 +\right.$$

$$6\left(h_1-h_2\right)^3\left(F+h_1-h_2\right)\left(-8B_1+A_1\left(h_1-h_2\right)\right)We +$$

$$a_9 = 40A_1^2We^2\left(-12\left(F+h_1-h_2\right)+B_1\left(h_1-h_2\right)^3 We\right)$$

Received : Apr. 10, 2011 ; Accepted :Oct. 16, 2012

REFERENCES

[1] Abd El Hakeem Abd El Naby, A.E.M. El Misery, M.F., Abd El Kareem, Separation in the Flow Through Peristaltic Motion of a Carreau Fluid in Uniform Tube, *Physica A*, **343**, p. 1 (2004).

[2] Mekheimer Kh. S., Peristaltic Flow of Blood under Effect of a Magnetic Field in a Non-Uniform Channels, *Appl. Math. Comp.*, **153**, p. 763 (2008).

[3] Kothandapani M., Srinivas S., Peristaltic Transport of a Jeffrey Fluid under the Effect of Magnetic Field in an Asymmetric Channel, *Int. J. Non-LinearMech.*, **43**, p. 915 (2008).

[4] Nadeem S., Akram Safia, Peristaltic Flow of a Williamson Fluid in an Asymmetric Channel, Commun. Nonlinear, *Sci. Numer. Simulat.* **15**, p. 1705 (2010).

[5] Nadeem S., Akram Safia, Peristaltic Transport of a Hyperbolic Tangent Fluid Model in an Asymmetric Channel, *Z. Naturforsch.*, **64a**, p. 559 (2009).

[6] Hayat T., Ellahi R., Asghar S., Unsteady Magnetohydrodynamic Non-Newtonian Flow Due to Non-Coaxial Rotations of a Disk and a Fluid at Infinity, *Chem.l Eng. Commun.*, **194**, p. 37 (2007).

[7] Rao A.R., Mishra M., Peristaltic Transport of a Ppower-Law Fluid in a Porous Tube, *J. Non-Newtonian Fluid Mech.*, **121**, p. 163 (2004).

[8] Yıldırım A., Sezer S.A., Effects of Partial Slip on the Peristaltic Flow of a MHD Newtonian Fluid in an Asymmetric Channel, *Math. and Comput. Model.* **52**, p. 618 (2010).

[9] Srinivas S., Kothandapani M., The Influence of Heat and Mass Transfer on MHD Peristaltic Flow Through a Porous Space with Compliant Walls, *Appl. Math. Comput.*, Doi 10.1016/j.amc. (2009).

[10] Eckert E.R.G., Drake R.M., "Analysis of Heat and Mass Transfer", McGraw-Hill, New York, (1972).

[11] Nadeem S., Noreen Sher Akbar, Influence of Radially Varying MHD on the Peristaltic Flow in an Annulus with Heat and Mass Transfer, *Taiw. Institute. Chem.Enging*. Doi: 10.1016/ j.jtice (2009).

[12] Nadeem S., Noreen Sher Akbar, Naheeda Bibi, Sadaf Ashiq, Influence of Heat and Mass Transfer on Peristaltic Flow of a Third Order Fluid in a Diverging Tube, *Commun. Nonlinear. Sci. Numer. Simulat.*, Doi: 10.1016/j.cnsns. (2009).

[13] S. Nadeem, Noreen Sher Akbar, Influence of Heat and Mass Transfer on a Peristaltic Motion of a Jeffrey-Six Constant Fluid in an Annulus, *Heat Mass Transf.*, DOI : $10.1007/s00231-010-0585-7$, (2010) .